Electronic Supplementary Information

# Bifunctional nickel oxide based nanosheets for highly efficient overall urea splitting

Fengchi Wu,[ab] Gang Ou,[ab] Jun Yang,[c] Henan Li,*[d] Yanxia Gao,[e] Fuming Chen,[f] Ye Wang[g] and Yumeng Shi*[ab]

[a] International Collaborative Laboratory of 2D Materials for Optoelectronics Science and Technology of Ministry of Education, College of Optoelectronic Engineering, Shenzhen University, Shenzhen 518060, China. E-mail: yumeng.shi@szu.edu.cn

[b] Engineering Technology Research Center for 2D Material Information Function Devices and Systems of Guangdong Province, College of Optoelectronic Engineering, Shenzhen University, Shenzhen 518060, China.

[c] Department of General Education, Army Engineering University of PLA, Nanjing 211101, China.

[d] College of Electronic Science and Technology, Shenzhen University, Shenzhen 518060, China. E-mail: henan.li@szu.edu.cn

[e] College of Physics and Optoelectronic Engineering, Shenzhen University, Shenzhen 518060, China.

[f] School of Physics and Telecommunication Engineering, South China Normal University, Guangzhou 510006, China.

[g] Key Laboratory of Material Physics of Ministry of Education, School of Physics and Engineering, Zhengzhou University, Zhengzhou 450052, China.

**Contents:**

**Fig. S12** UOR, HER and overall urea splitting property of NFO microspheres with and without XC-72R: (a,b) LSV and EIS curves of UOR, (c,d) LSV and EIS curves of HER, (e) LSV curves for overall urea splitting.

**Fig. S13** CV curves of (a) NO and (b) NFO microspheres at different scan rates (10, 20, 30, 40 and 50 mV $s^{-1}$).

**Fig. S14** The currents of NO and NFO microspheres at 0.05 V vs. Ag/AgCl plotted as a function of scan rates.

**Fig. S15** The ECSA of NO and NFO microspheres.

**Fig. S16** The overall urea splitting activity of NO and NFO microspheres by ECSA.

**Fig. S17** Crystal structures of (a) NO and (c) NFO and calculated band structures of (b) NO and (d) NFO.

**Table S1**. Resistance of NO and NFO for UOR.

**Table S2**. Resistance of NO and NFO for HER.

**Table S3**. Comparison of urea electrocatalytic property in 1 M KOH at 10 mA $cm^{-2}$.

**Table S4**. Resistance of NFO with and without XC-72R for HER and UOR.

## EXPERIMENTAL SECTION

**Synthesis of NO and NFO hollow microspheres.** The nickel oxide based microspheres were synthesized by coprecipitation method. In brief, 20 mmol $Ni(NO_3)_2 \cdot 6H_2O$ (99.99%, Sigma Aldrich) was dissolved in 50 ml deionized water. The solution was kept stirring at 70 °C. Then, 50 ml of 1 M dilute ammonia water was gradually added in it at a drop rate of 5 ml $min^{-1}$ and stirred at 70 °C for 30 minutes. The product was harvested by centrifugation at 10000 rpm for 5 minutes and thoroughly washed 3 times by deionized water to remove the impurity ions. After that, the product was dried at 80 °C for 5 h then calcined at 450 °C for 2 h in air at heating rate of 5 °C $min^{-1}$. NFO hollow microspheres were also prepared by the same method by using 18 mmol $Ni(NO_3)_2$ together with 2 mmol $Fe(NO_3)_3 \cdot 9H_2O$ (99.95%, Sigma Aldrich) as substrates.

**Physical characterization.** The crystal structure was characterized by X-ray diffraction (XRD, D/max-2500, Rigaku). The morphology and elemental mapping were performed by scanning electron microscopy (SEM, JSM-7001F, JEOL). The microstructure was analyzed by transmission electron microscopy (TEM, JEM-2010, JEOL). The specific surface area (SSA) was measured by surface area analyzer (Quadra Sorb SI, Quantachrome). The elemental chemical state was measured by X-ray photoelectron spectrometer (XPS, Escalab 250Xi, Thermo Fisher Scientific).

**Electrochemical characterization.** The electrocatalytic urea splitting properties of NO and NFO were tested by electrochemical workstation (CHI-760E, CH Instrument). UOR and HER properties were characterized by a three-electrode system, where

Ag/AgCl was used as the reference electrode, Pt sheet and carbon rod were used as counter electrode for OER/UOR and HER, respectively. The working electrode was fabricated by dropping the evenly dispersed mixture of oxide powders, Nafion 117 (Aldrich), and ethanol on the carbon fiber paper (CFP) and dried naturally with catalyst loading of 0.5 mg $cm^{-2}$. The HER performance of commercial Pt/C (10%, JM) and OER and UOR performance of commercial $IrO_2$ (99.9%, Aladdin) were also measured by the same method for comparison. The test solution was 1 M KOH with or without 0.33 M urea. The scanning rate of linear scanning voltammetry (LSV) was 5 mV $s^{-1}$. The test potential of electrochemical impedance spectroscopy (EIS) was 0.35 V and -1.125 V vs Ag/AgCl for UOR and HER, respectively, while frequency range was 100k~0.1 Hz. Urea splitting performance of NO and NFO were characterized by two-electrode method. LSV analysis was implemented in the same way as mentioned above. The stability of the material was tested by chronopotentiometry at current density of 10 mA $cm^{-2}$. Cyclic voltammetry (CV) was applied to measure the electrochemically active surface area (ECSA) in a non-faradic range of 0-0.1 V vs. Ag/AgCl at scan rate of 10-50 mV $s^{-1}$. All LSV curves were corrected with 95% iR-compensation. All the tests were performed at room temperature.

**Calculation Details.** All first-principles calculations were performed based on the DFT using CASTEP code with plane-wave pseudoptential total energy scheme method. The electronic exchange correlation interactions were processed using the LDA, the average force acting on ions was reduced to $1.0\times10^{-6}$ eV $atom^{-1}$. The mean

Hellmann-Feynman force acting on each atom was 0.01 eV $A^{-1}$. Convergence tests with respect to k mesh point (4×4×4) and kinetic energy cutoff were performed (500 eV) for all crystals.

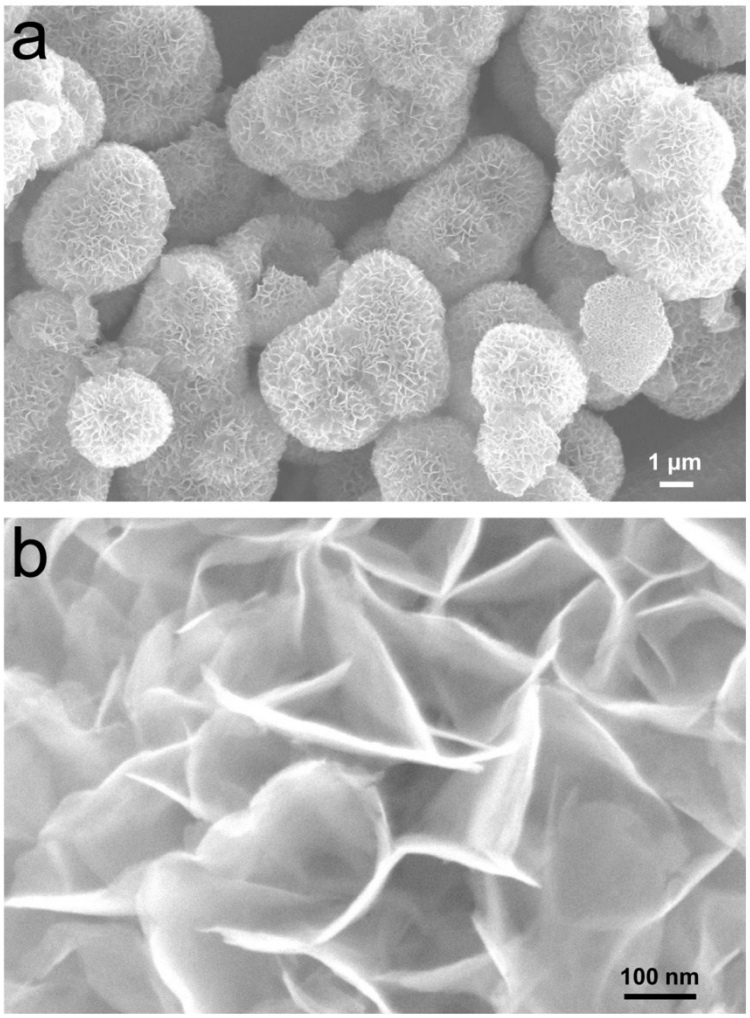


**Fig. S1** SEM images of NO microspheres at (a) low magnification and (b) high magnification.

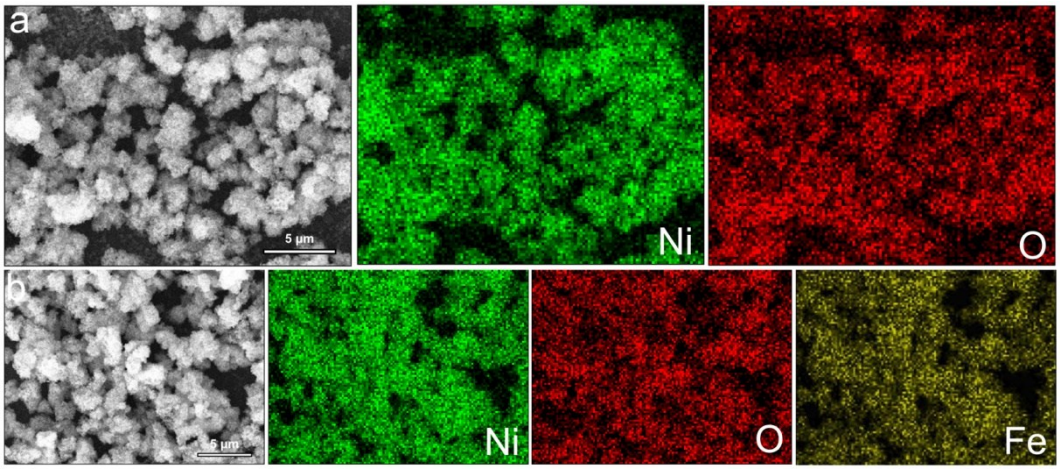


**Fig. S2** Elemental mapping analysis of (a) NO and (b) NFO microspheres.

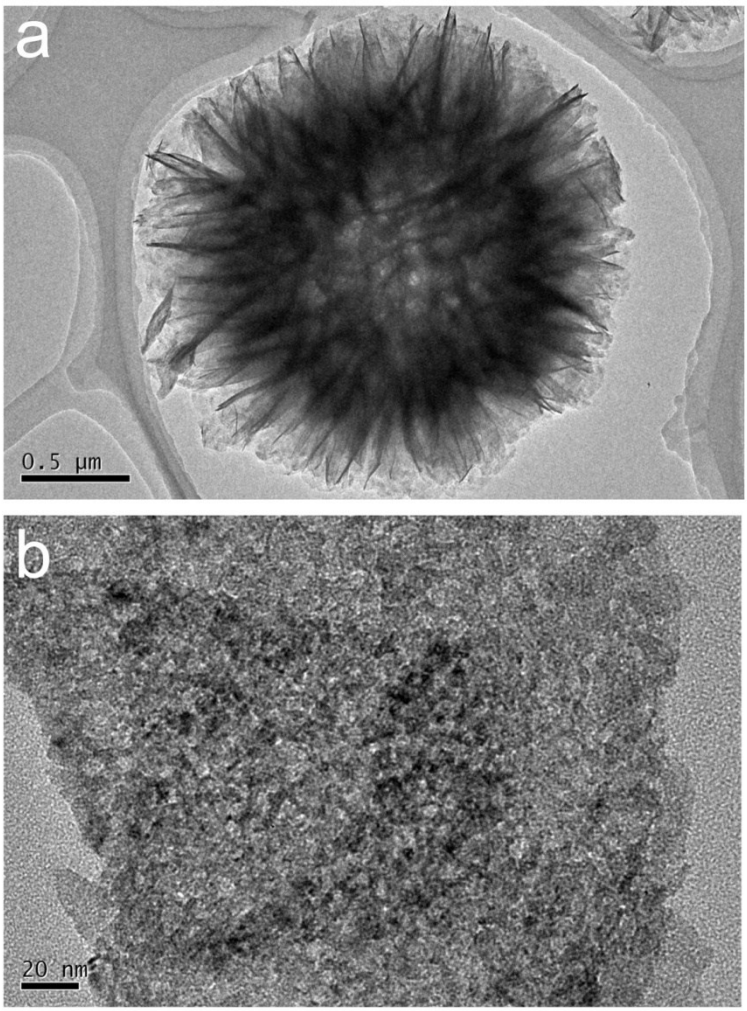


**Fig. S3** TEM images of NO microsphere at (a) low magnification and (b) high magnification.

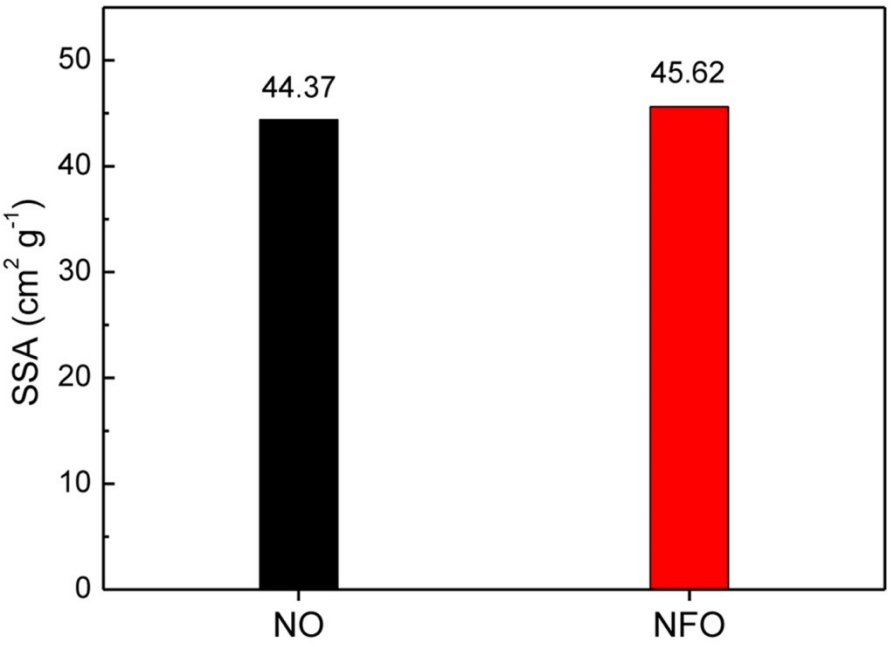


**Fig. S4** Specific surface areas of NO and NFO microspheres.

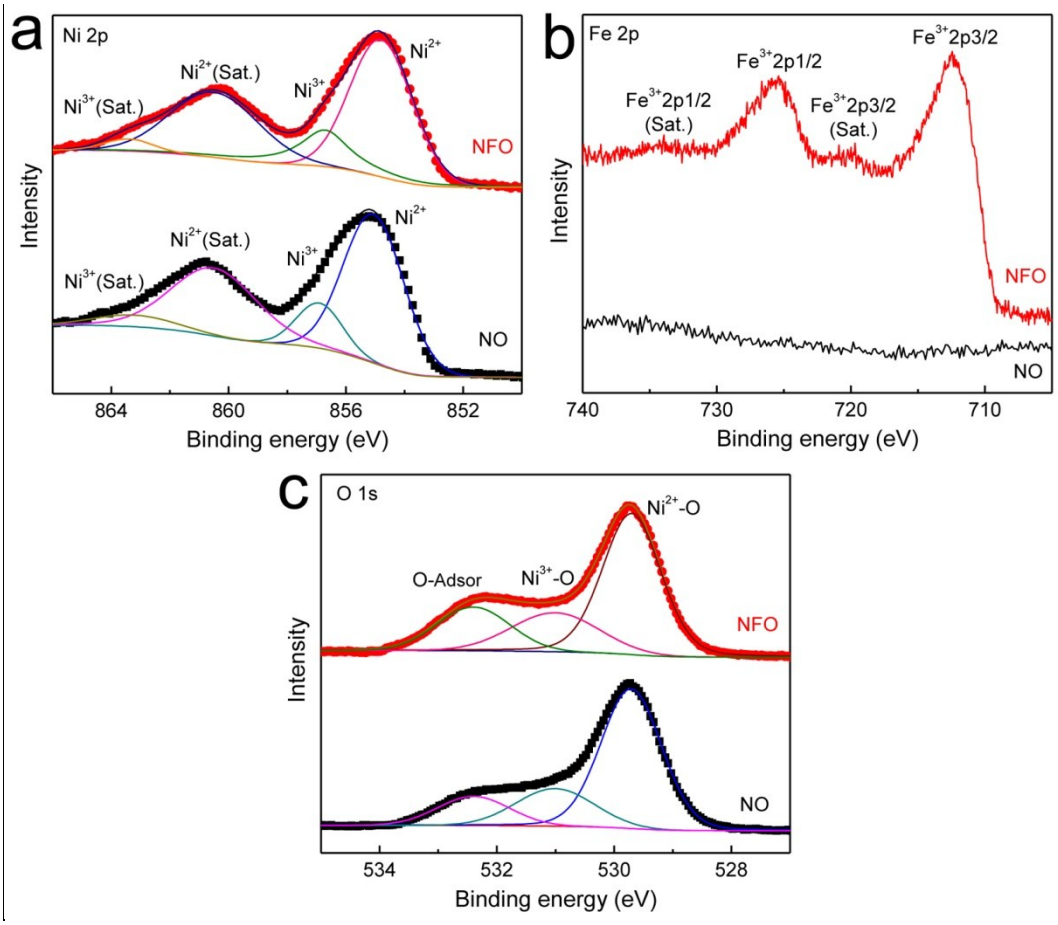


**Fig. S5** XPS spectra of NO and NFO microspheres: (a) Ni 2p, (b) Fe 2p, (c) O 1s.

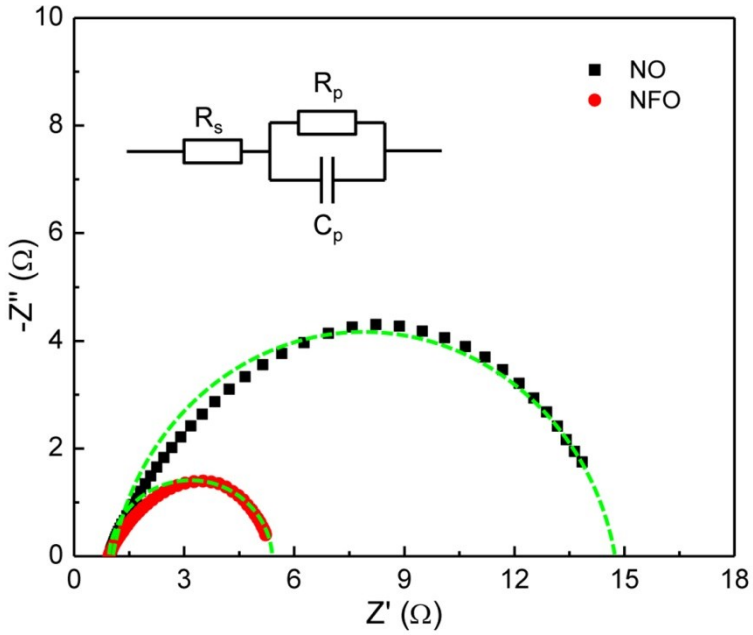


**Fig. S6** EIS spectra of NO and NFO in 1 M KOH with 0.33 M urea.

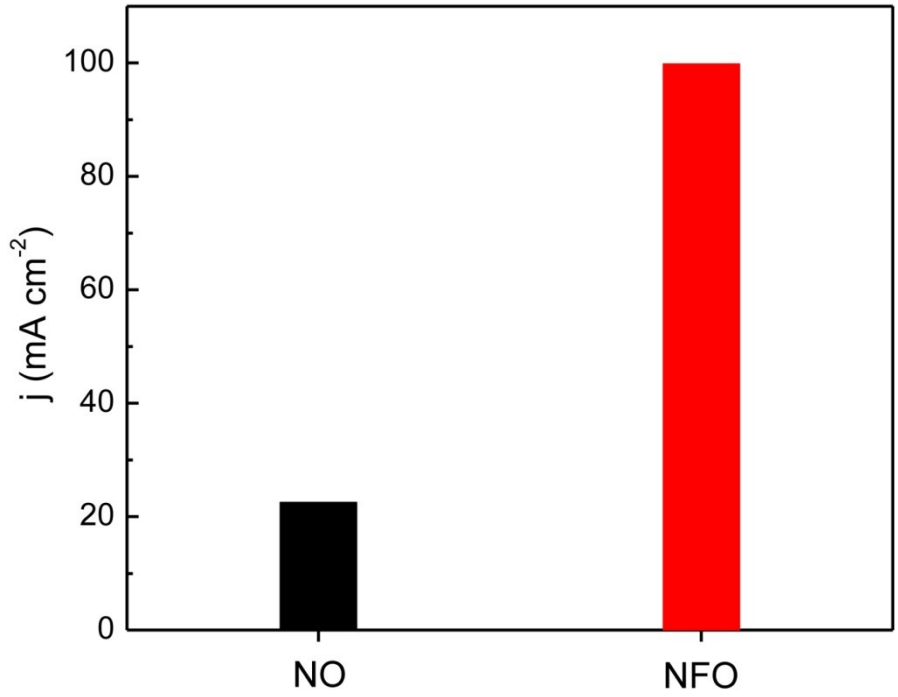


**Fig. S7** UOR current density of NO and NFO at 1.4 V vs RHE with 0.33 M urea.

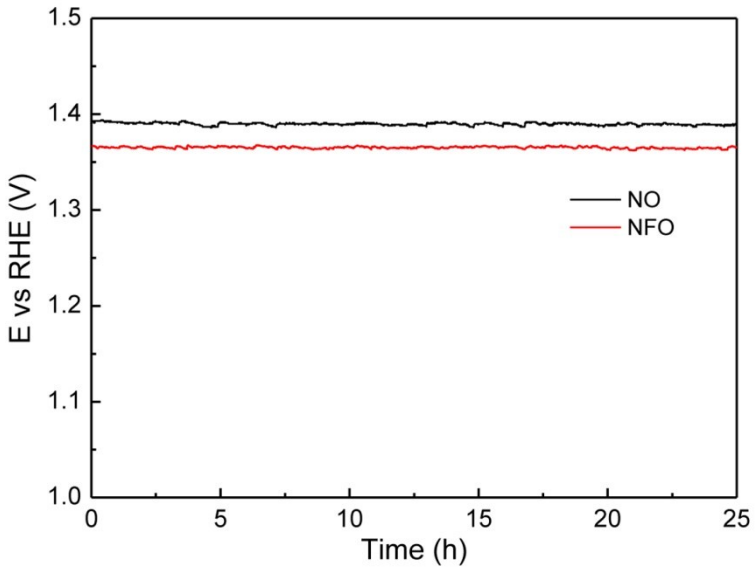


**Fig. S8** Chronopotentiometry curves of NO and NFO microspheres for UOR at current density of 10 mA $cm^{-2}$.

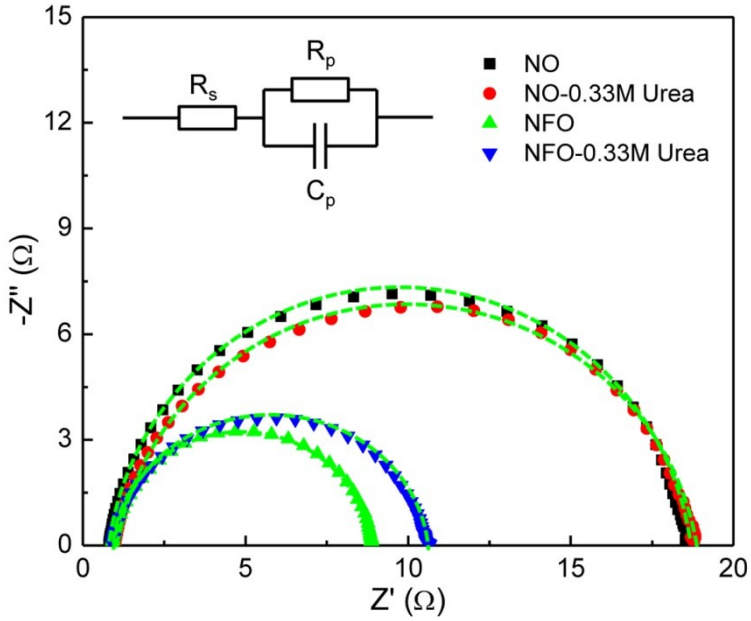


**Fig. S9** EIS spectra of NO and NFO in 1 M KOH with and without 0.33 M urea.

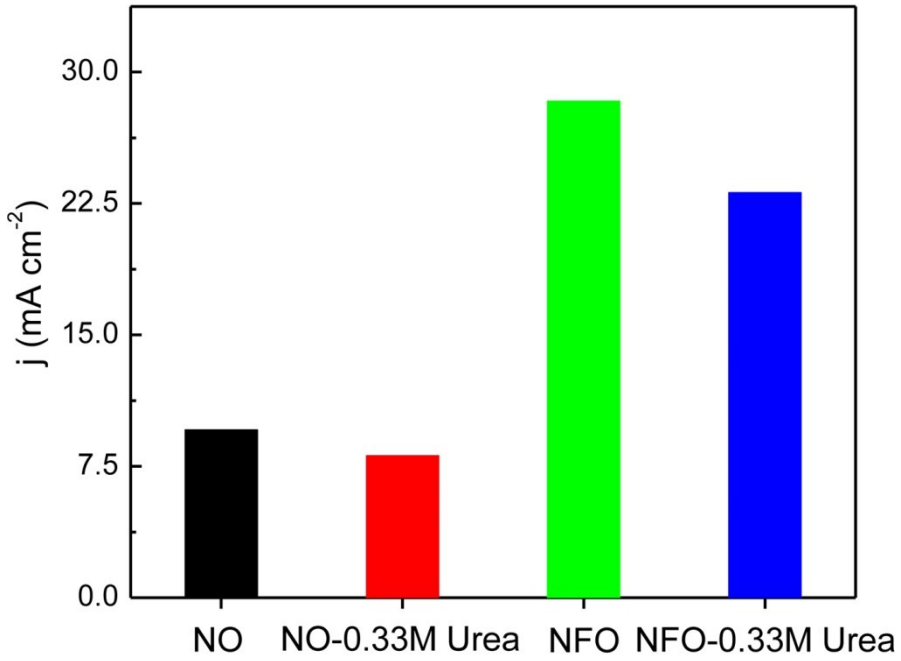


**Fig. S10** HER current density of NO and NFO at -0.1 V vs RHE with and without 0.33 M urea.

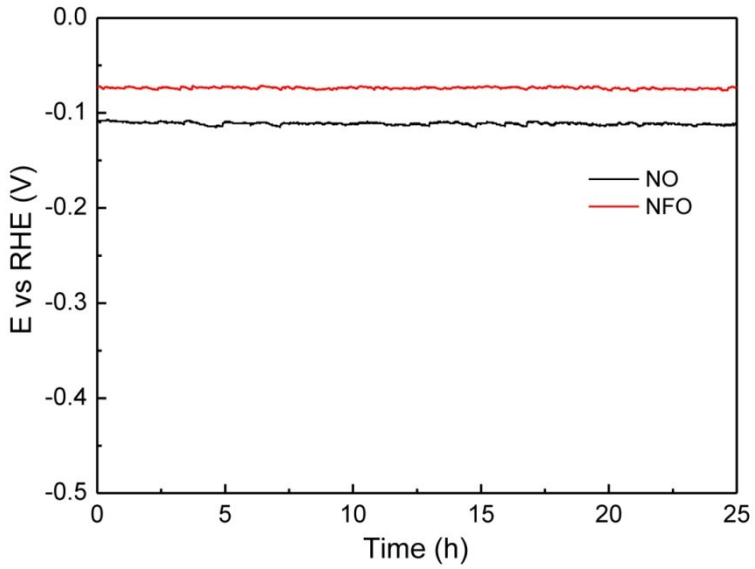


**Fig. S11** Chronopotentiometry curves of NO and NFO microspheres for HER at current density of 10 mA $cm^{-2}$.

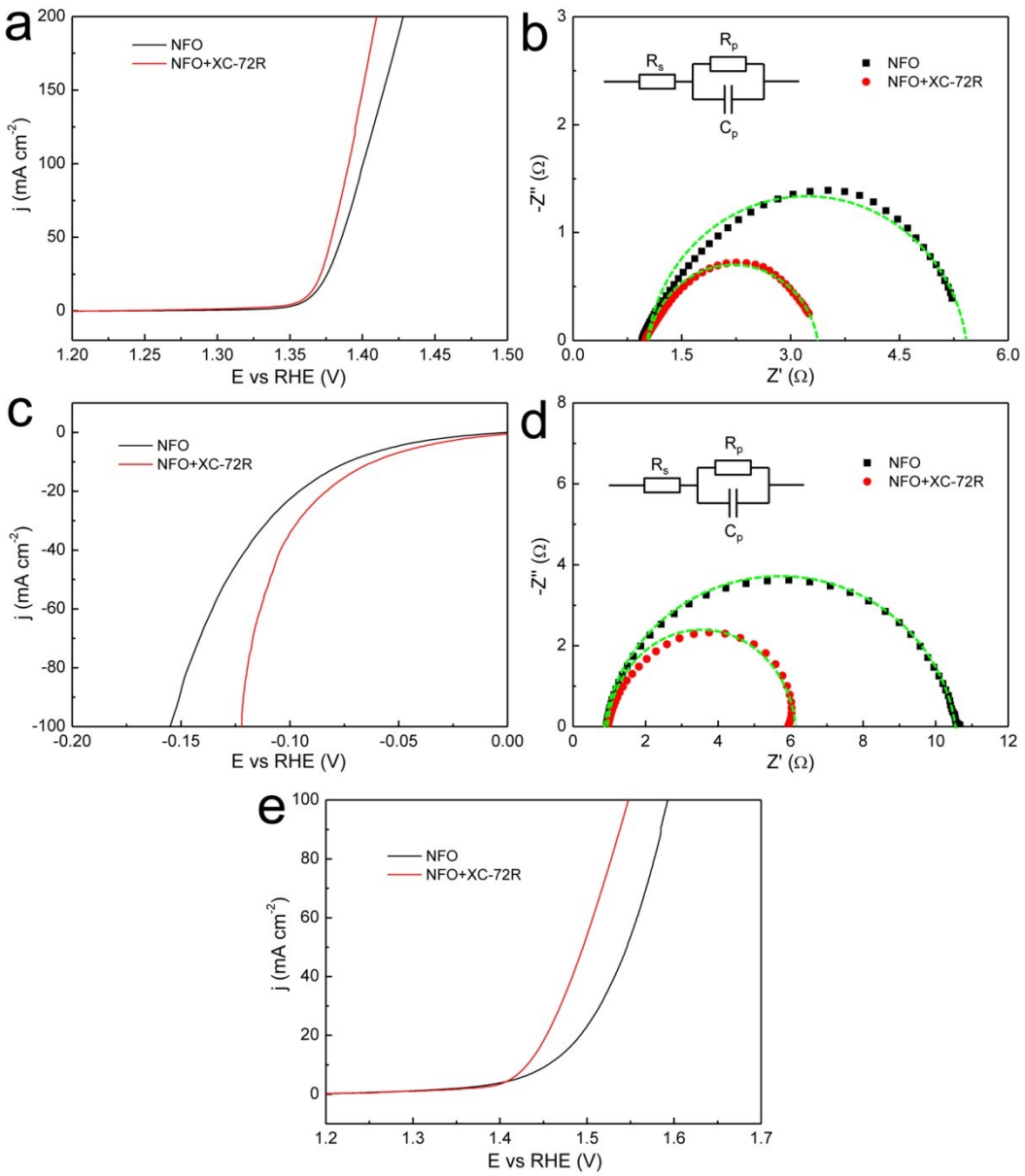


**Fig. S12** UOR, HER and overall urea splitting property of NFO microspheres with and without XC-72R: (a,b) LSV and EIS curves of UOR, (c,d) LSV and EIS curves of HER, (e) LSV curves for overall urea splitting.

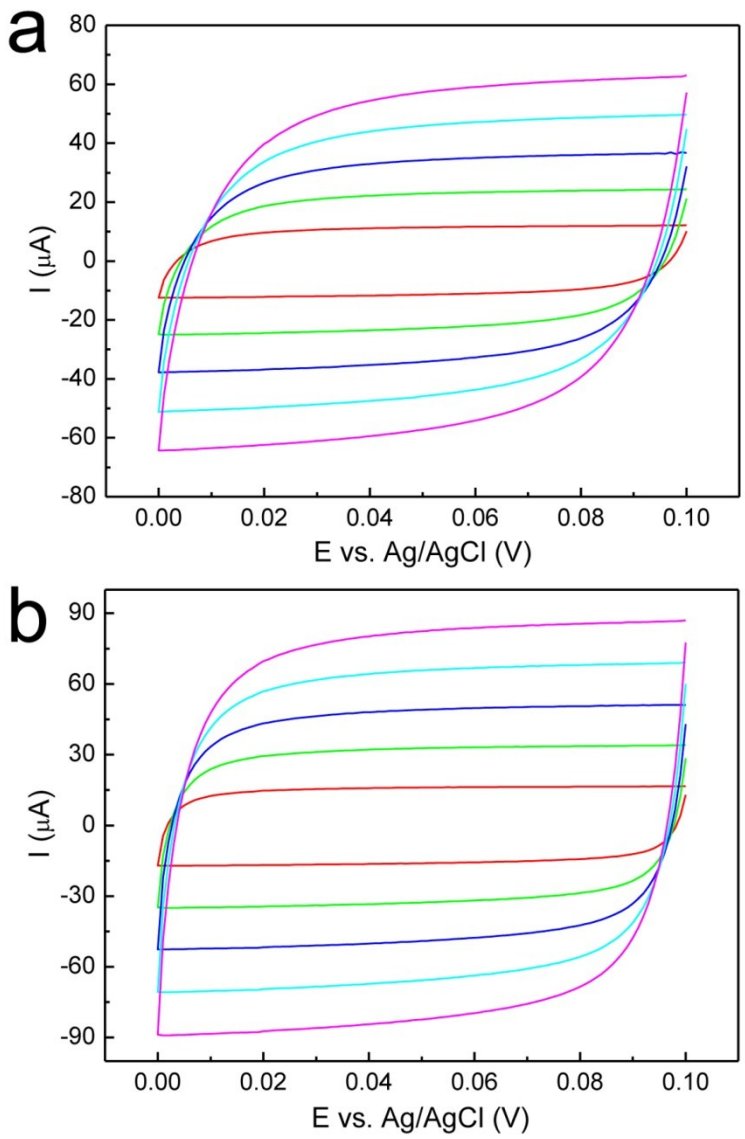


**Fig. S13** CV curves of (a) NO and (b) NFO microspheres at different scan rates (10, 20, 30, 40 and 50 mV $s^{-1}$).

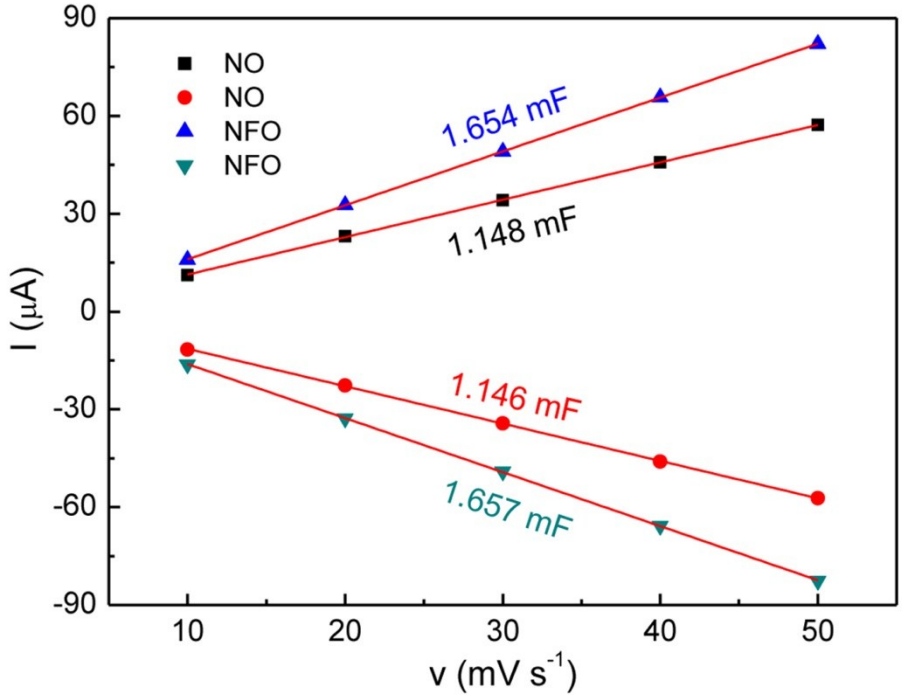


**Fig. S14** The currents of NO and NFO microspheres at 0.05 V vs. Ag/AgCl plotted as a function of scan rates.

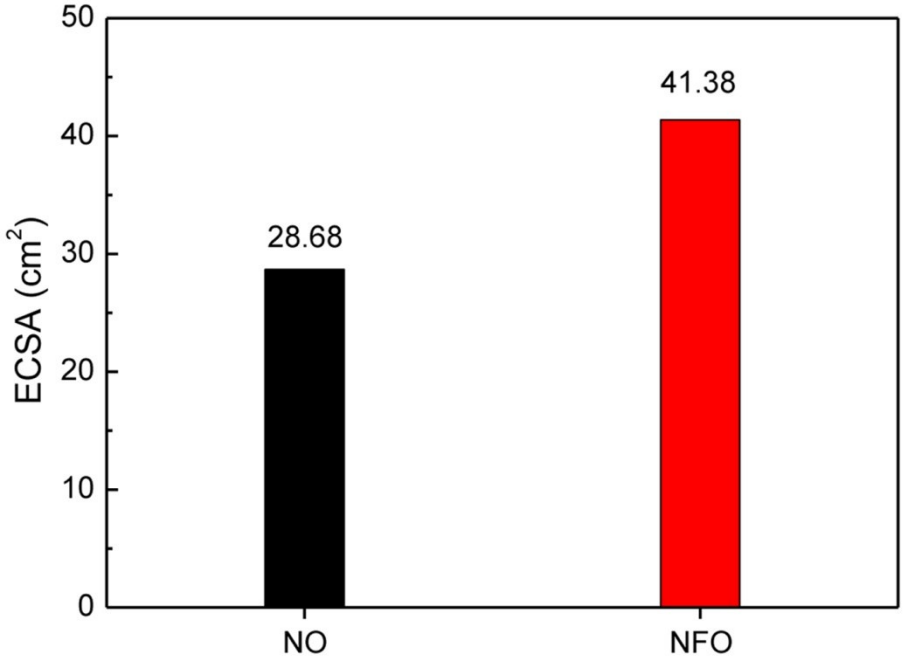


**Fig. S15** The ECSA of NO and NFO microspheres.

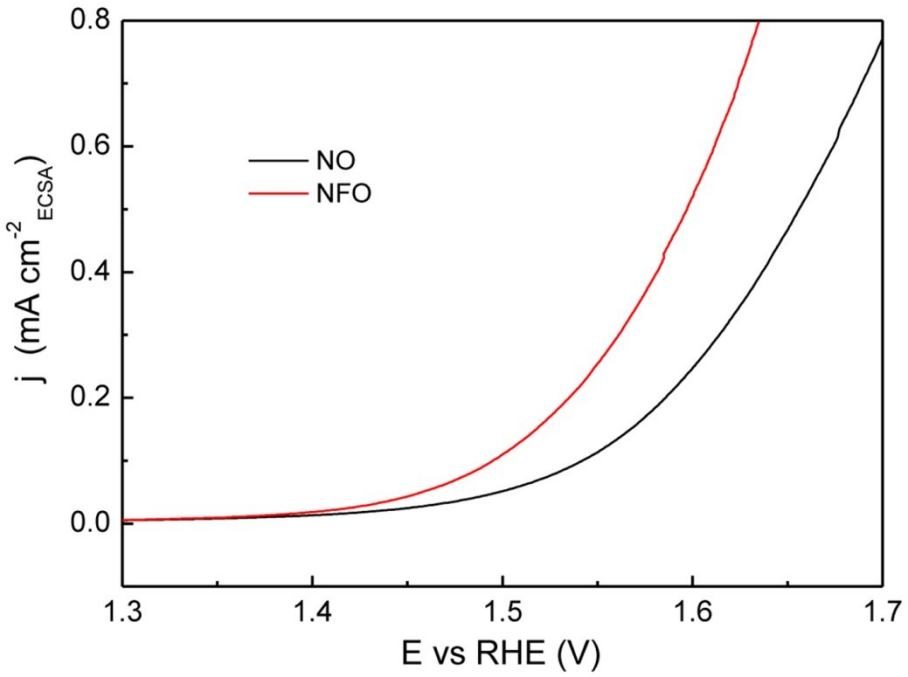


**Fig. S16** The overall urea splitting activity of NO and NFO microspheres by ECSA.

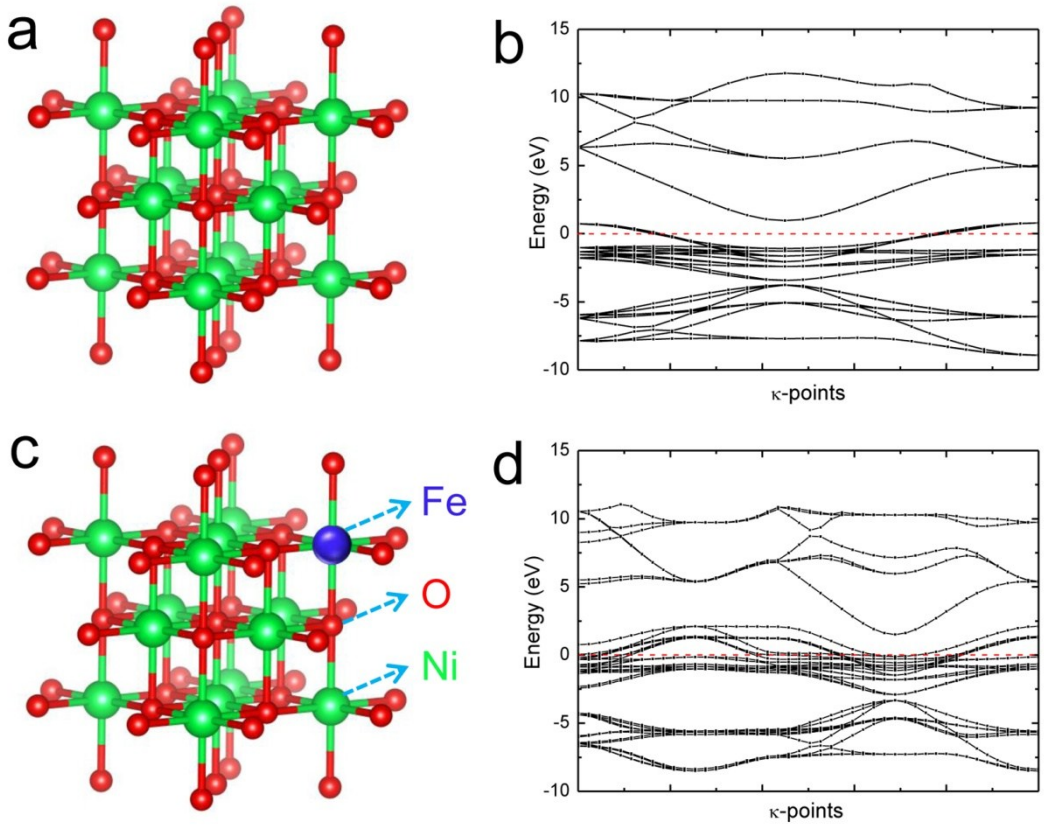


**Fig. S17** Crystal structures of (a) NO and (c) NFO and calculated band structures of (b) NO and (d) NFO.

**Table S1**. Resistance of NO and NFO for UOR.

| Resistance (Ω) | NO | NFO |
|---|---|---|
| $R_s$ | 1.0 | 1.0 |
| $R_p$ | 13.8 | 4.4 |

**Table S2**. Resistance of NO and NFO for HER.

| Resistance (Ω) | Without 0.33 M Urea | | With 0.33 M Urea | |
|---|---|---|---|---|
| | NO | NFO | NO | NFO |
| $R_s$ | 0.9 | 0.9 | 0.9 | 0.9 |
| $R_p$ | 17.6 | 7.9 | 17.9 | 9.7 |

**Table S3**. Comparison of urea electrocatalytic property in 1 M KOH at 10 mA $cm^{-2}$.

| Catalyst | Urea (M) | UOR (V) | HER (mV) | Urea splitting (V) | Ref. |
|---|---|---|---|---|---|
| NFO | 0.33 | 1.365 | -72 | 1.455 | This work |
| $V_{Ni}$-α-$Ni(OH)_{2-x}$ | 0.33 | 1.398 | N | N | [1] |
| $LaNiO_3$ | 0.33 | 1.376 | N | N | [2] |
| Ni/C | 0.33 | 1.388 | -40 | 1.6 | [3] |
| NiFe DH/NF | 0.33 | 1.45 | N | N | [4] |
| Ni-MOF | 0.33 | 1.36 | N | N | [5] |
| $Ni_3N$ NA/CC | 0.33 | 1.35 | -136 | 1.44 | [6] |
| M-$Ni(OH)_2$ NS | 0.33 | 1.39 | N | N | [7] |
| NiMoO/NF | 0.5 | 1.37 | -11 | 1.38 | [8] |
| HC-NiMoS/Ti | 0.5 | 1.37 | -122 | 1.59 | [9] |
| $MnO_2$/$MnCo_2O_4$/NF | 0.5 | 1.425 | -277 | 1.55 | [10] |
| r-$NiMoO_4$/NF | 0.5 | 1.365 | N | N | [11] |
| $Ni(OH)_2$ NS/NF | 0.6 | 1.425 | N | N | [12] |

**Table S4**. Resistance of NFO with and without XC-72R for HER and UOR.

| Resistance (Ω) | HER | | UOR | |
|---|---|---|---|---|
| | NFO | NFO+XC-72R | NFO | NFO+XC-72R |
| $R_s$ | 0.9 | 0.9 | 1.0 | 1.0 |
| $R_p$ | 9.7 | 5.2 | 4.4 | 2.3 |

References:


1 Q. He, Y. Y. Wan, H. L. Jiang, Z. W. Pan, C. Q. Wu, M. Wang, X. J. Wu, B. J. Ye, P. M. Ajayan and L. Song, *ACS Energy Lett.*, 2018, **3**, 1373.

2 R. P. Forslund, J. T. Mefford, W. G. Hardin, C. T. Alexander, K. P. Johnston and K. J. Stevenson, *ACS Catal.*, 2016, **6**, 5044.

3 L. Wang, L. T. Ren, X. R. Wang, X. Feng, J. W. Zhou and B. Wang, *ACS Appl. Mater. Inter.*, 2018, **10**, 4750.

4 W. Xu, D. W. Du, R. Lan, J. Humphreys, Z. C. Wu and S. W. Tao, *New J. Chem.*, 2017, **41**, 4190.

5 D. D. Zhu, C. X. Guo, J. L. Liu, L. Wang, Y. Du and S. Z. Qiao, *Chem. Commun.*, 2017, **53**, 10906.

6 Q. Liu, L. S. Xie, F. L. Qu, Z. A. Liu, G. Du, A. M. Asiri and X. P. Sun, *Inorg. Chem. Front.*, 2017, **4**, 1120.

7 X. J. Zhu, X. Y. Dou, J. Dai, X. D. An, Y. Q. Guo, L. D. Zhang, S. Tao, J. Y. Zhao, W. S. Chu, X. C. Zeng, C. Z. Wu and Y. Xie, *Angew. Chem. Int. Ed.*, 2016, **55**, 12465.

8 Z. Y. Yu, C. C. Lang, M. R. Gao, Y. Chen, Q. Q. Fu, Y. Duan and S. H. Yu, *Energ. Environ. Sci.*, 2018, **11**, 1890.

9 X. X. Wang, J. M. Wang, X. P. Sun, S. Wei, L. Cui, W. R. Yang and J. Q. Liu, *Nano Res.*, 2018, **11**, 988.

10 C. L. Xiao, S. N. Li, X. Y. Zhang and D. R. MacFarlane, *J. Mater. Chem. A*, 2017, **5**, 7825.

11 Y. Tong, P. Z. Chen, M. X. Zhang, T. P. Zhou, L. D. Zhang, W. S. Chu, C. Z. Wu and Y. Xie, *ACS Catal.*, 2017, **8**, 1.

12 K. Ye, H. Y. Zhang, L. T. Zhao, X. M. Huang, K. Cheng, G. L. Wang and D. X. Cao, New J. Chem., 2016, 4, 8673.